金星大気の観測　これまで（風速以外）

今村(JAXA)

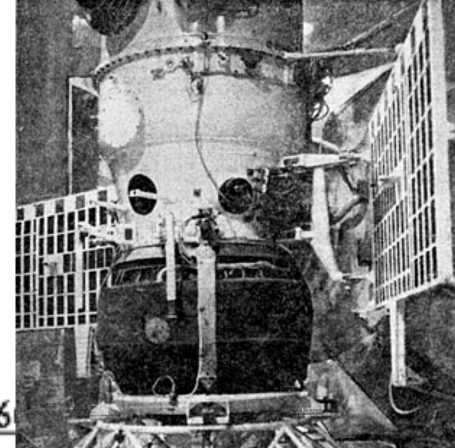

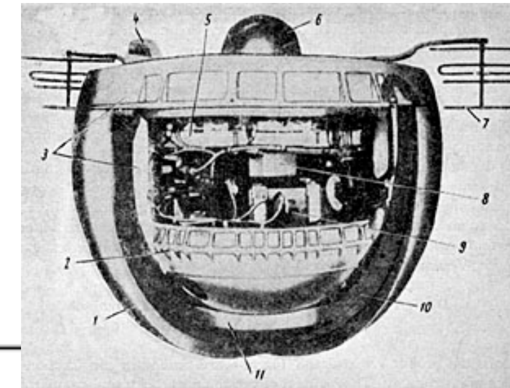

Venera-4 Descent Module (1967)

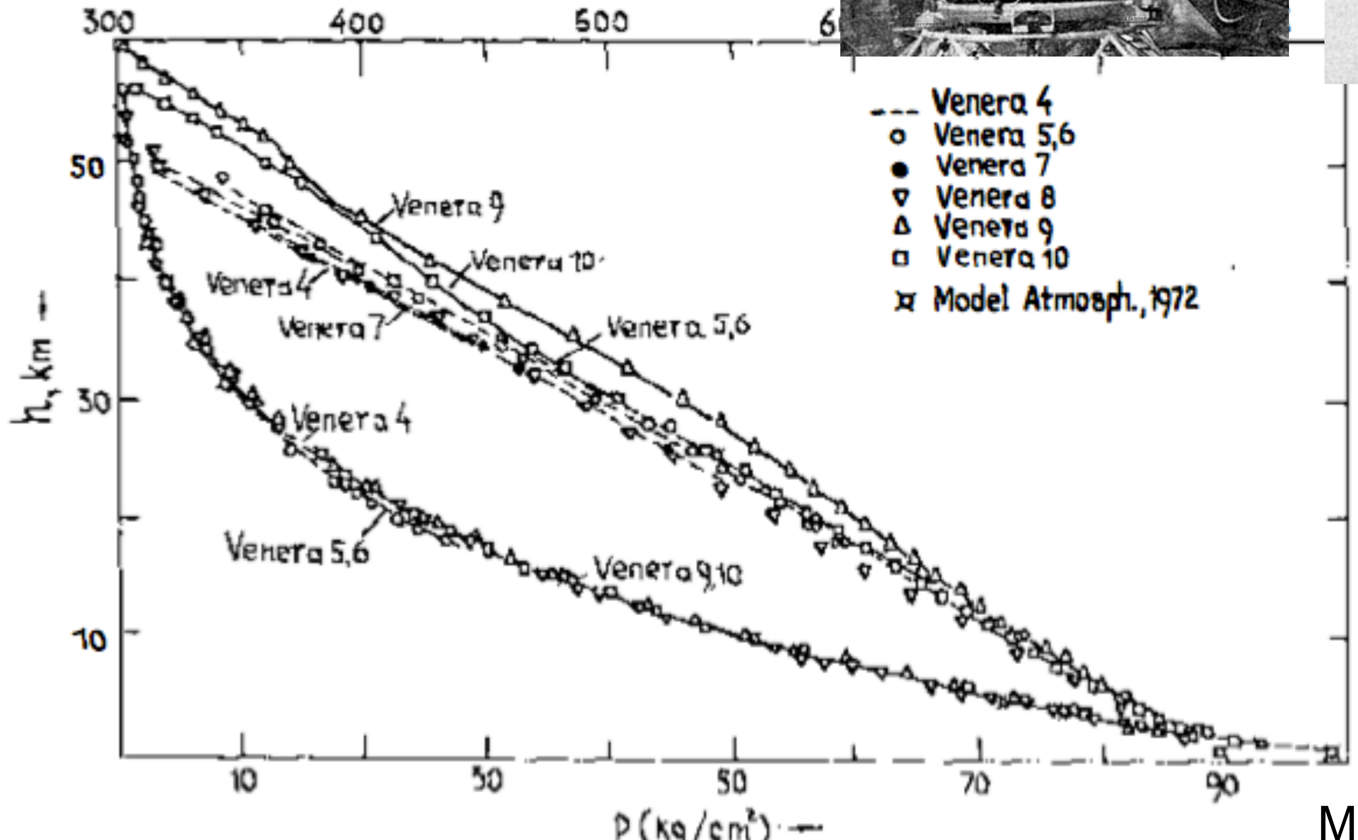

Marov (1978)

Figure 4 Atmospheric temperature and pressure variations
Venera 4–10 landers compared with the model distribution adopted in 1975 as the COSPAR Reference Model atmosphere. The model's surface position corresponds to planetary radius $R_♀ = 6050$ km.

able 4 Chemical composition of the Venus atmosphere

Component	Relative abundance (by volume)	Technique	References
CO_2	0.97 ± 0.03	Gas-analyzer Venera 4, 5, and 6	Vinogradov et al. 1968, 1970a, b
N_2 (+ noble gases)	<0.02	Venera 4, 5, and 6	Vinogradov et al. 1968, 1970a, b
H_2O	10^{-3}–10^{-2}	Venera 4, 5, and 6	Vinogradov et al. 1968, 1970a, b
	10^{-6}–10^{-5}	Ground-based spectroscopy	Schorn et al. 1969, Fink et al. 1972, Barker 1975
	3×10^{-4}	Ratio of H_2O and CO_2 bands intensities, Venera 9 and 10.	Moroz et al. 1976
	$<2 \times 10^{-3}$	Radio astronomy	Kuzmin & Marov 1974, Smirnova & Kuzmin 1974
CO	5×10^{-5}	Ground-based spectroscopy	Kuiper et al. 1967, Connes et al. 1968, Young, L. 1972
HCl	4×10^{-7}	Ground-based spectroscopy	Connes et al. 1967, Young, L. 1972
HF	10^{-8}	Ground-based spectroscopy	Connes et al. 1967, Young, L. 1972
NH_3	10^{-4}–10^{-3}	Gas-analyzer, Venera 8.	Surkov et al. 1973
	$<10^{-7}$	Ground-based spectroscopy	Kuiper et al. 1968–69
	$<10^{-5}$	Radio astronomy	Kuzmin & Marov 1974, Smirnova & Kuzmin 1974

Marov (1978)

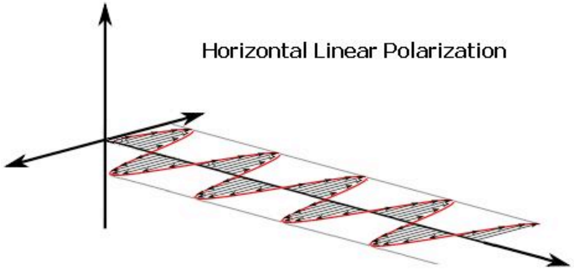

Polarization of sunlight reflected by Venus

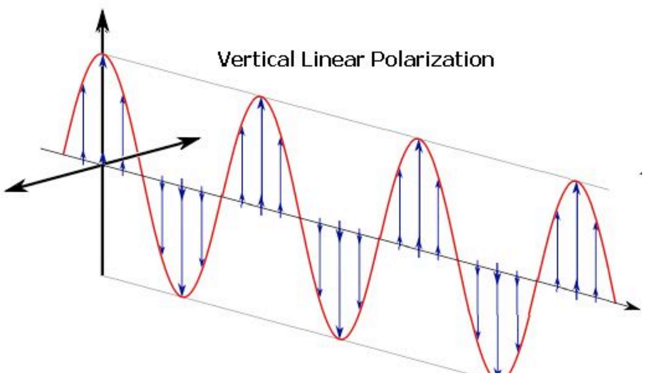

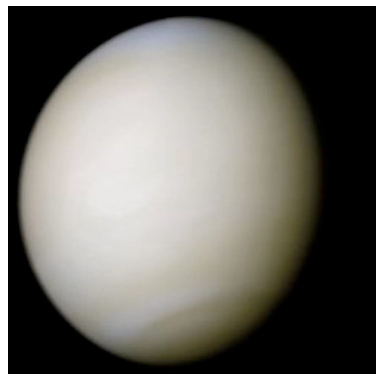

Hansen & Hovenier (1974)

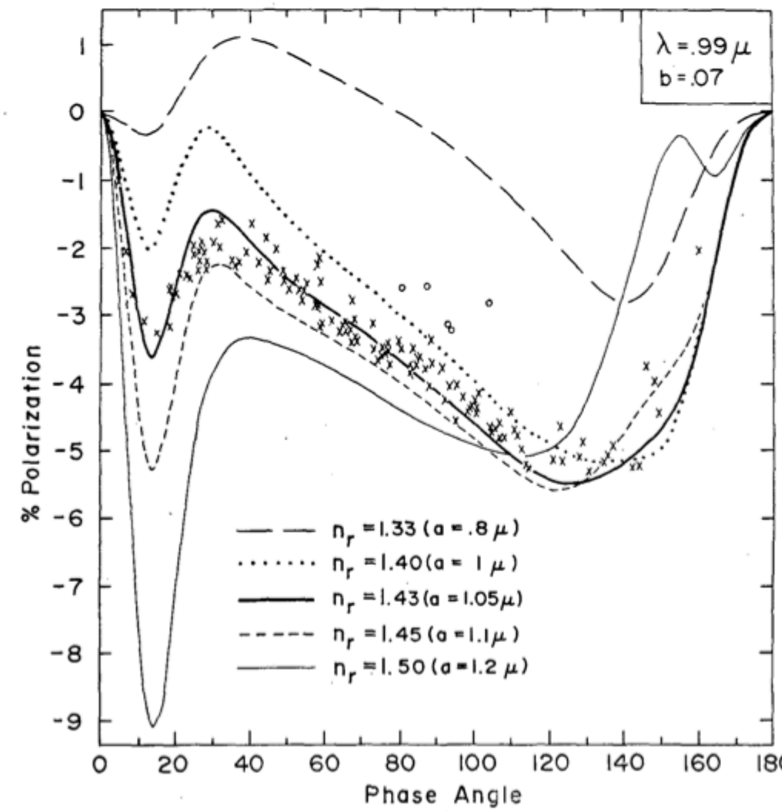

FIG. 7. Observations and theoretical computations of the polarization of sunlight reflected by Venus at $\lambda = 0.99$ μm. The observations were made with an intermediate bandwidth filter, the ×'s being obtained by Coffeen and Gehrels (1969) in 1959–67 and by Coffeen (cf. Dollfus and Coffeen, 1970) from 1967 to March 1969, and the ○'s being obtained by Coffeen (cf. Dollfus and Coffeen, 1970) in May–July, 1969. The theoretical curves are for spherical particles having the size distribution (8) with $b = 0.07$. The different theoretical curves are for various refractive indices, the effective particle radius being selected in each case to yield closest agreement with the observations for all wavelengths.

Refractive index = 1.44

→consistent with H_2SO_4-H_2O solution

Effective radius ~ 1 μm

Microphysical properties

- H_2SO_4-H_2O droplets with radii r < 5 μm
- Smallest mode (including sub-cloud haze) might be condensation nuclei whose composition is unknown.
- Size distribution is variable.

Knollenberg & Hunten (1980)

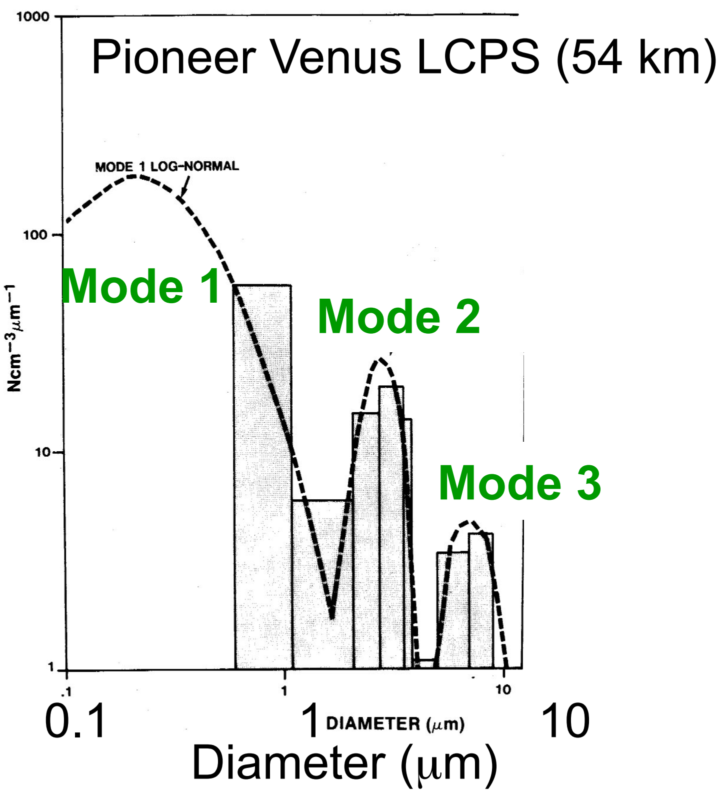

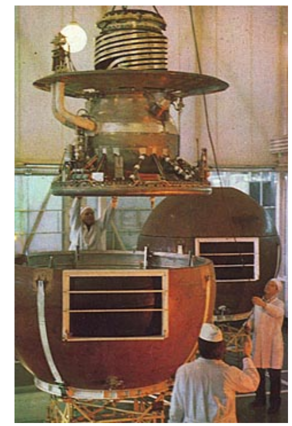

Venera-13 Lander

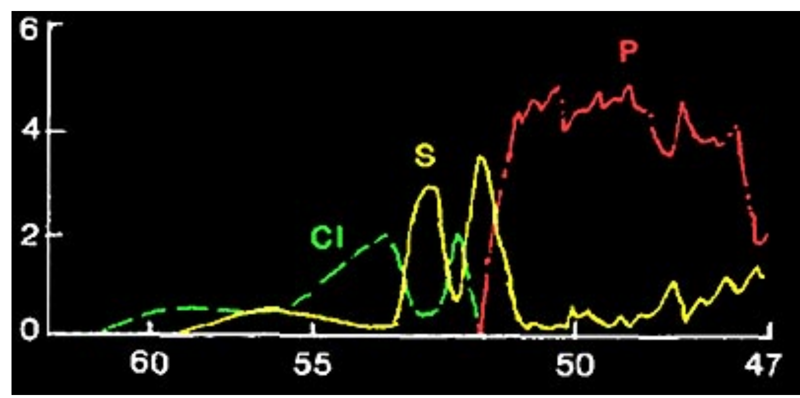

Cl ? S ? P ?

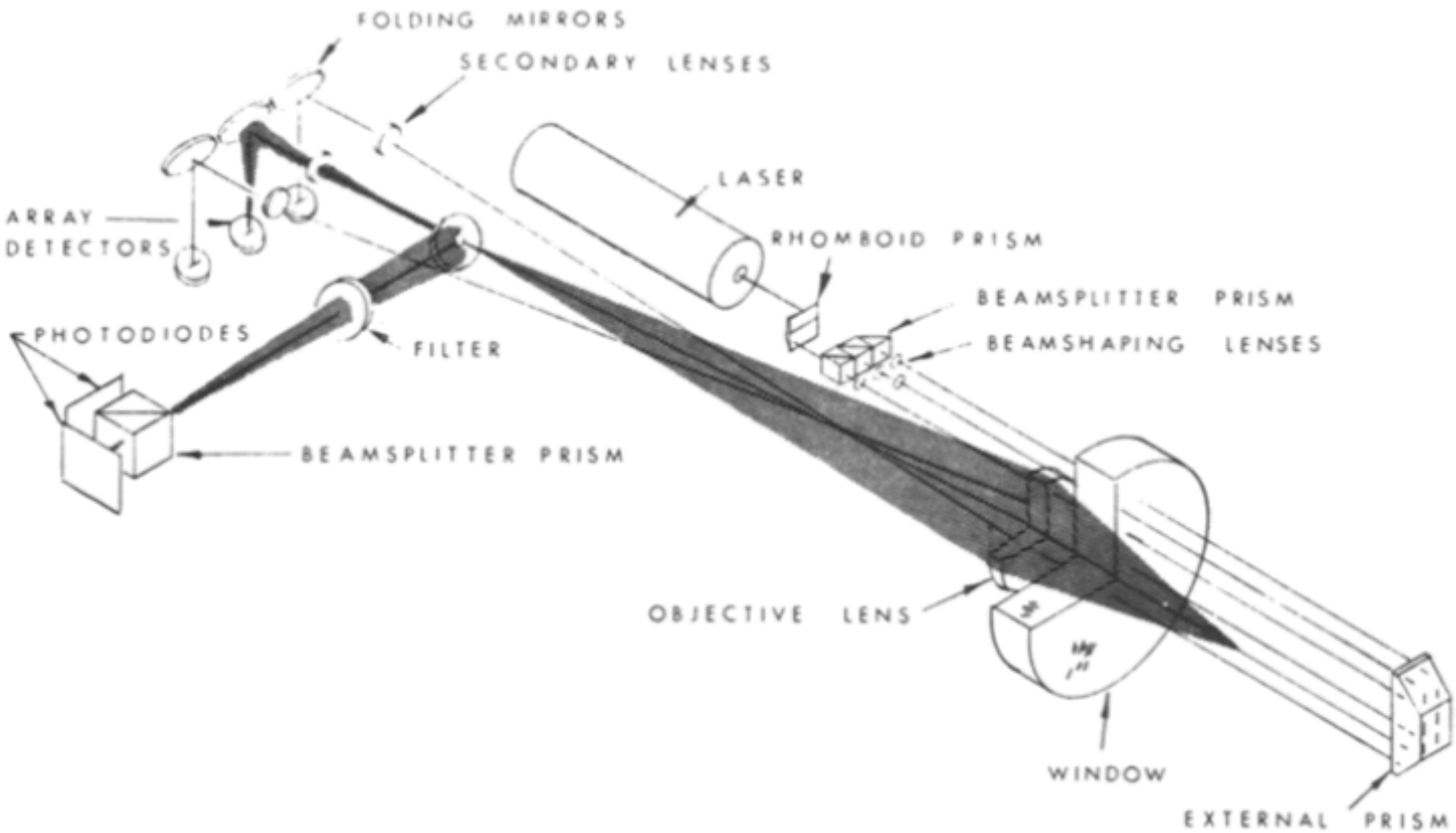

Fig. 11. (LCPS). LCPS optical diagram.

Microphysical properties

- H_2SO_4-H_2O droplets with radii r < 5 μm
- Smallest mode (including sub-cloud haze) might be condensation nuclei whose composition is unknown.
- Size distribution is variable.

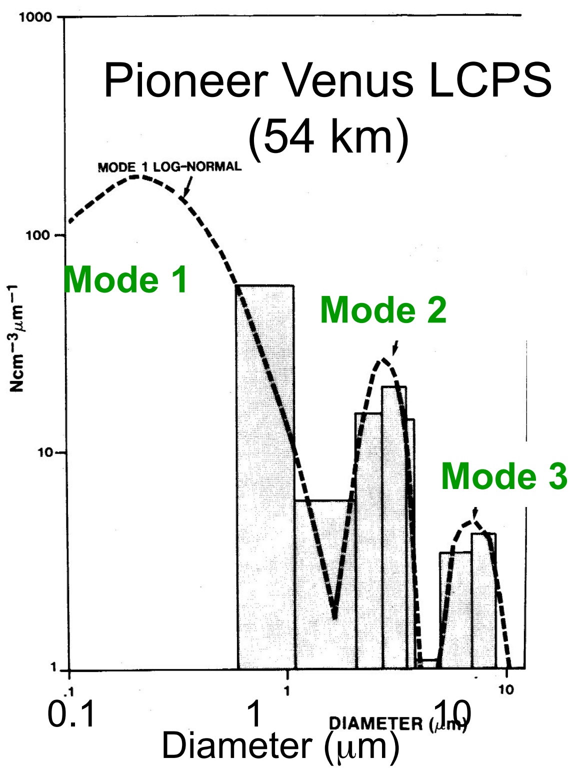

Knollenberg & Hunten (1980)

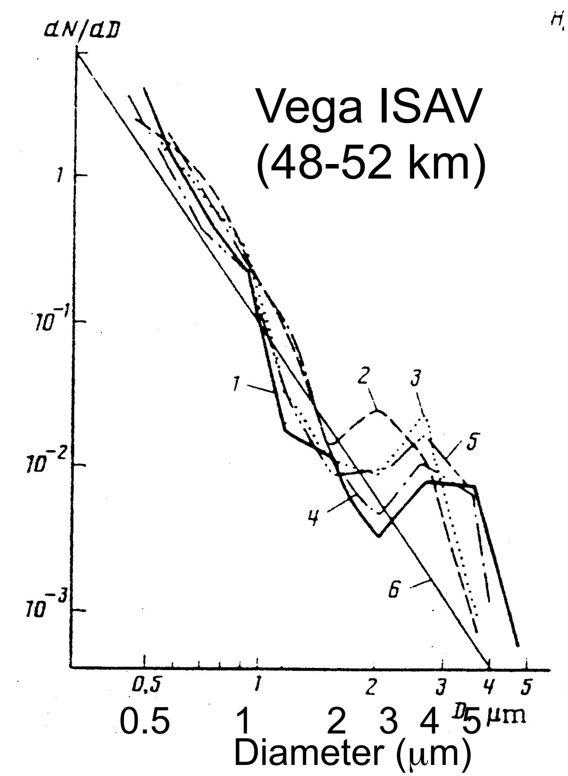

Gnedykh et al., 1987

Three-layered structure – Different dynamical and chemical regimes at different altitudes?

Pioneer Venus LCPS (Knollenberg and Hunten, 1980)

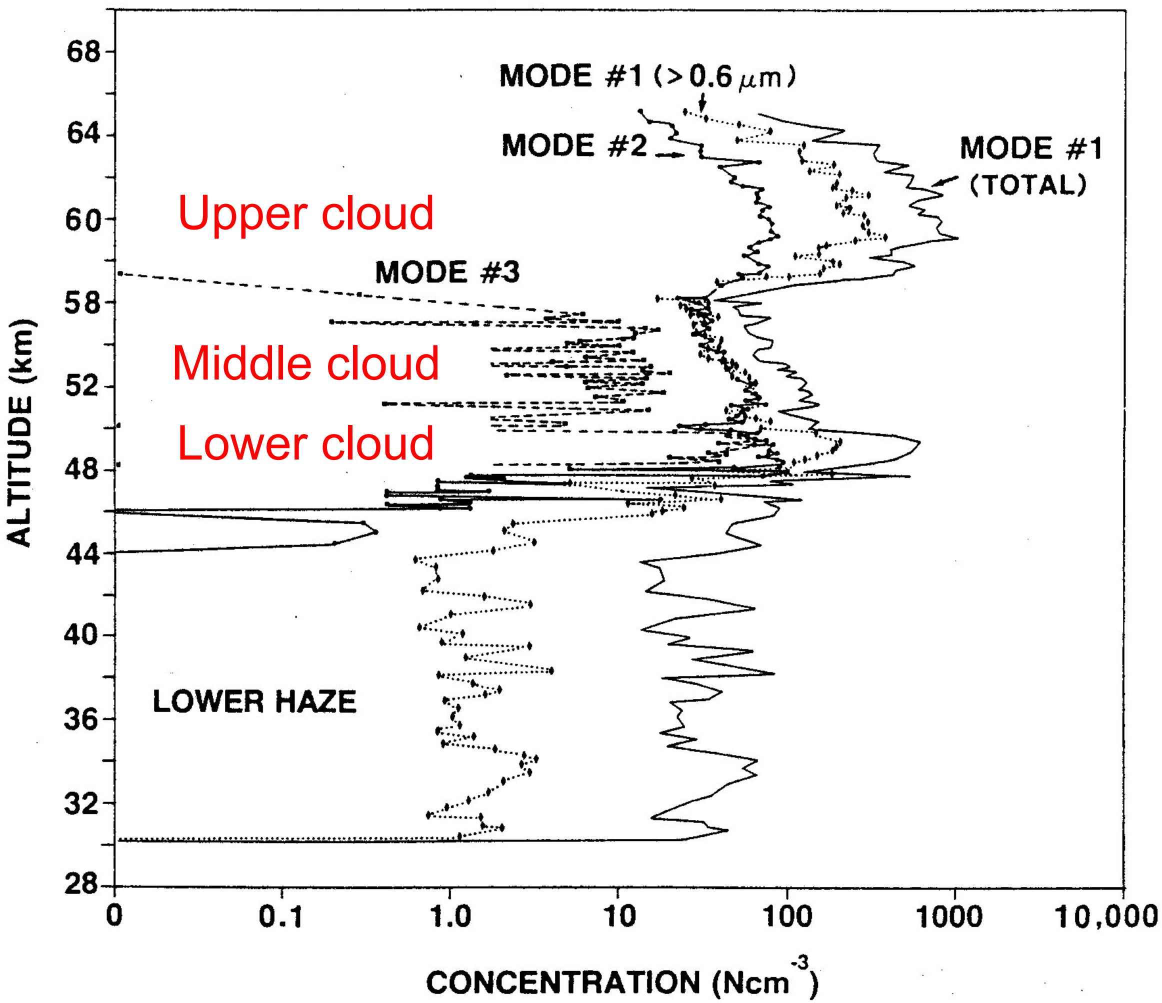

Static stability measured by entry probes

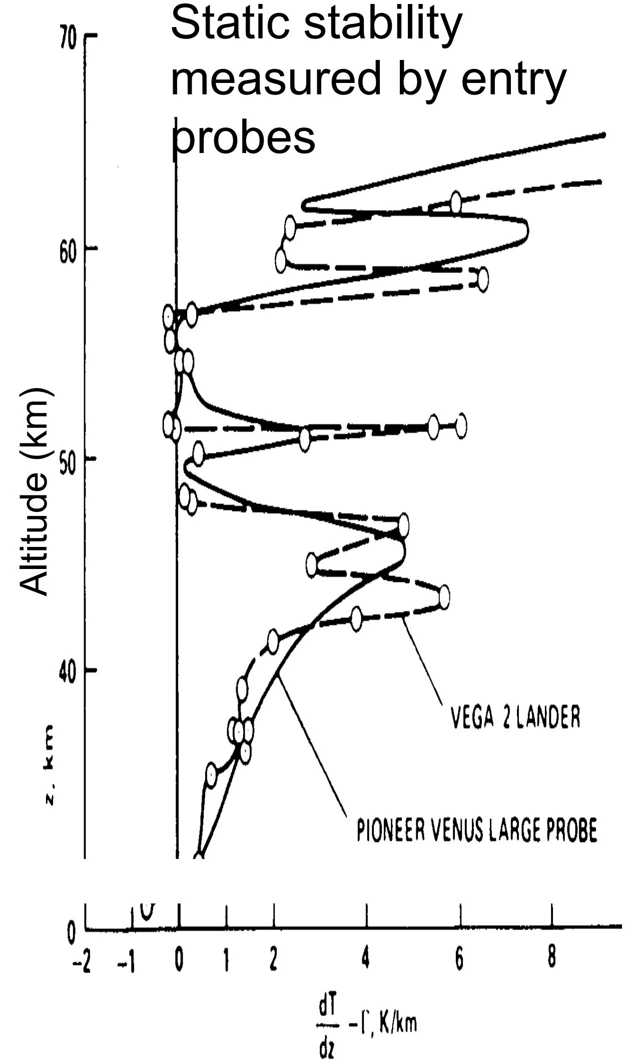

Sulfur-rich atmosphere: origin of H_2SO_4 ?

SO_2 measurements by Vega landers

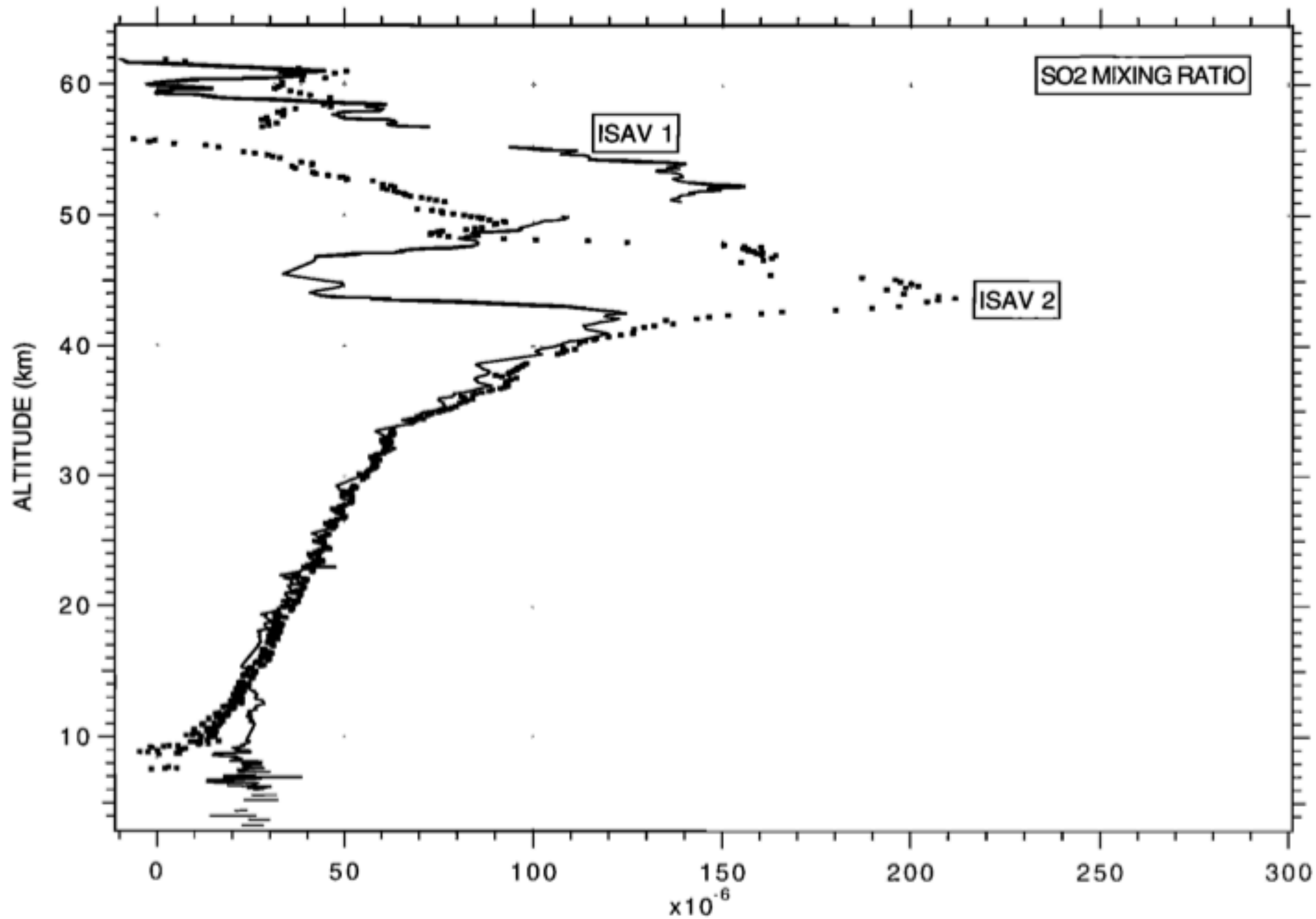

Figure 24. The SO_2 mixing ratio vertical profile retrieved for ISAV 2 (data points) is compared to that determined for ISAV 1. There is a large difference of structure above 40 km, while the profiles are nearly identical below 40 km. A peak of 210 ppm is observed at 43 km in the ISAV 2 data.

Bertaux et al. (1996)

H_2SO_4 vapor profiles

67°N by Magellan

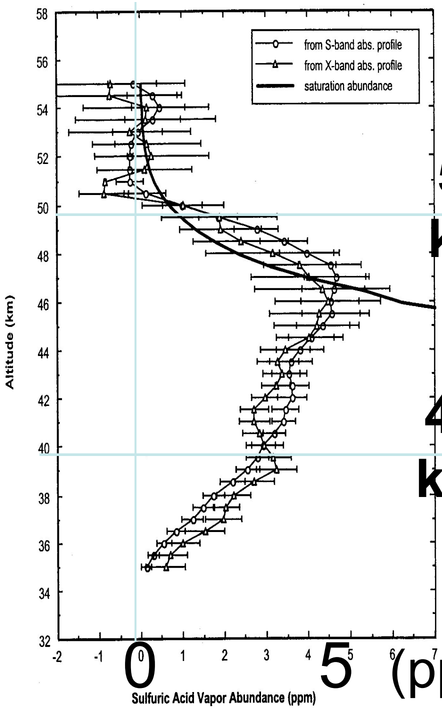

Equator by Mariner 10

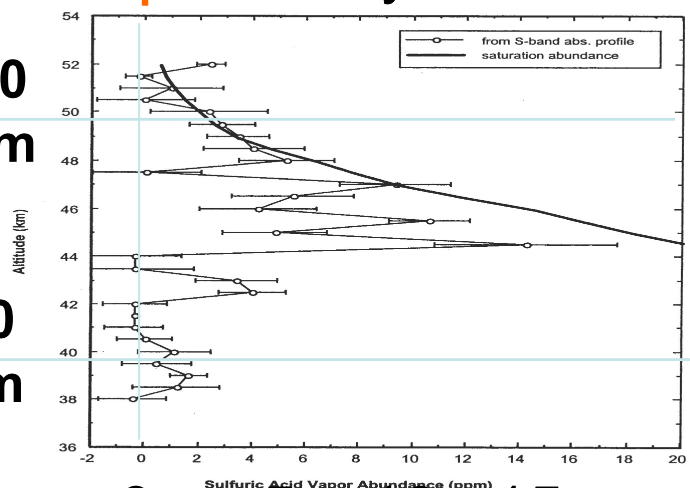

Kolodner & Steffes (1998)

by Pioneer Venus

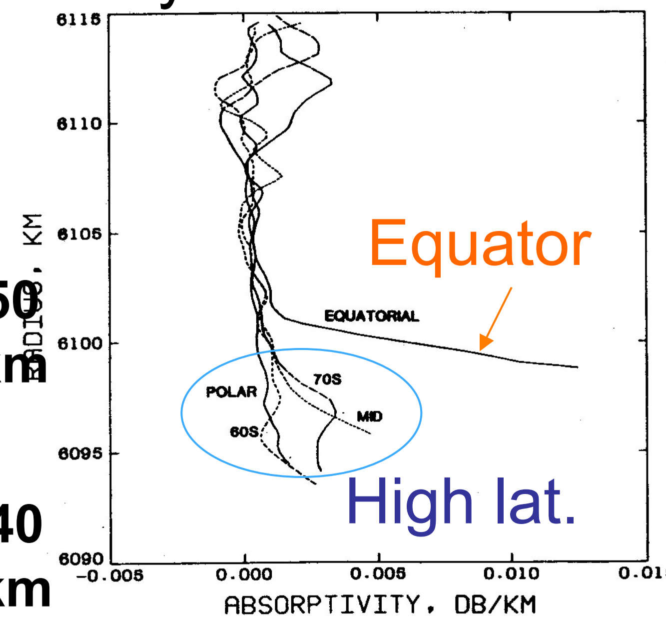

Jenkins & Steffes (1991)

Traditional 1D model

(Krasnopolsky & Pollack 1994; James et al. 1997)

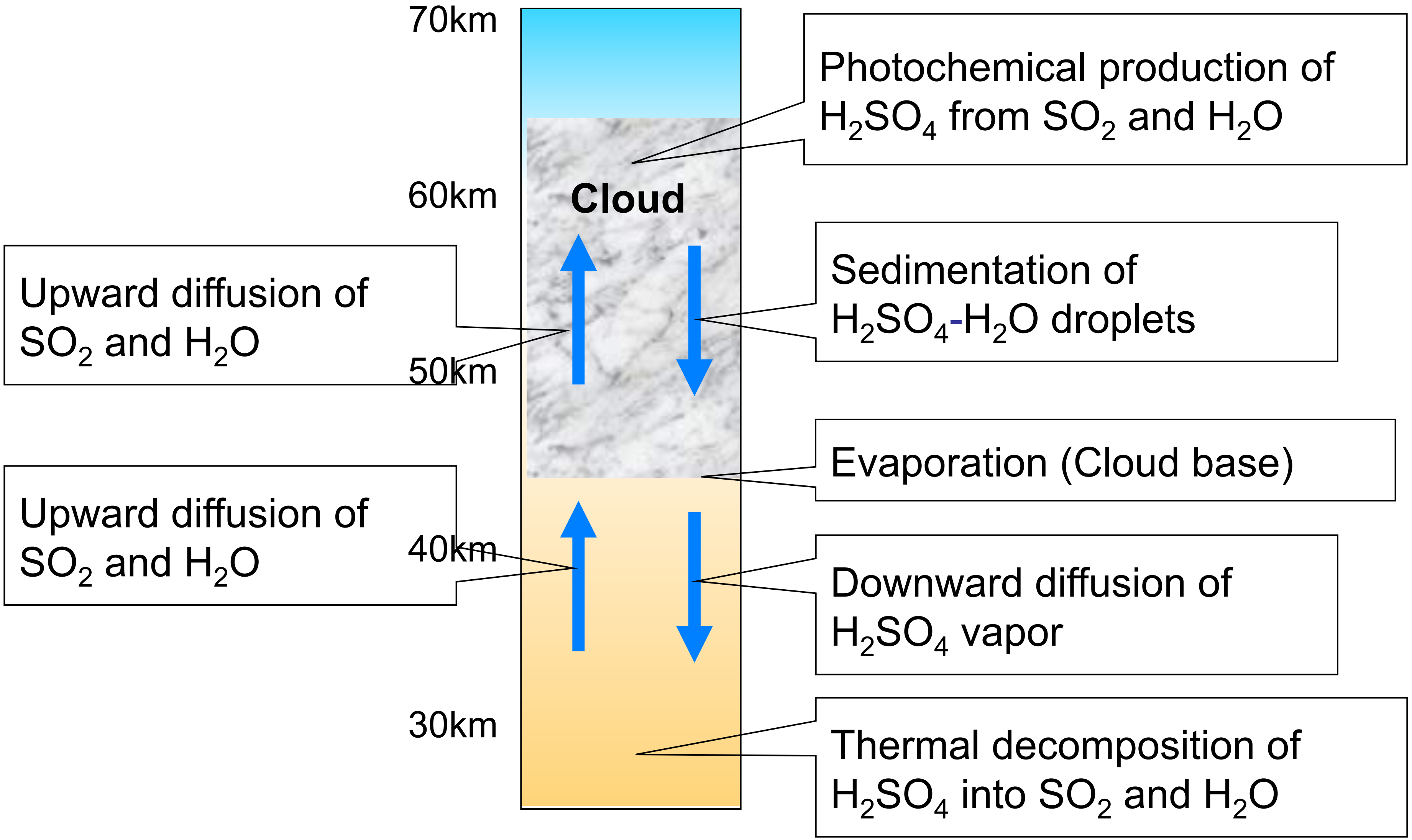

Ground-based observations of cloud-related gaseous species

f

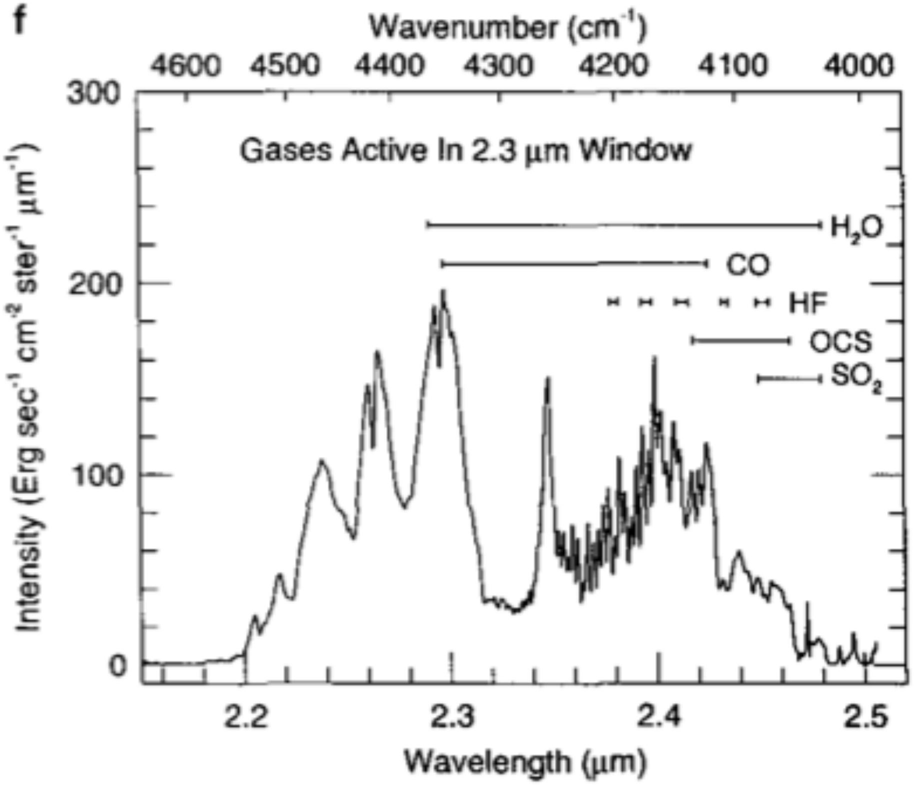

a

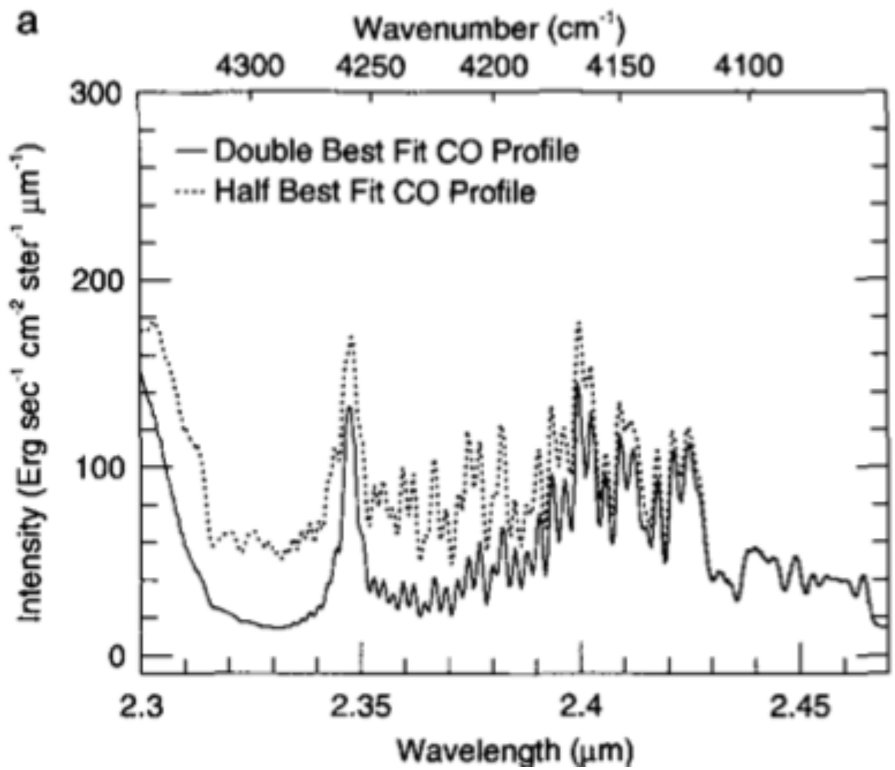

Pollack et al., Icarus 103, 1, 1993

Retrieved vertical profiles

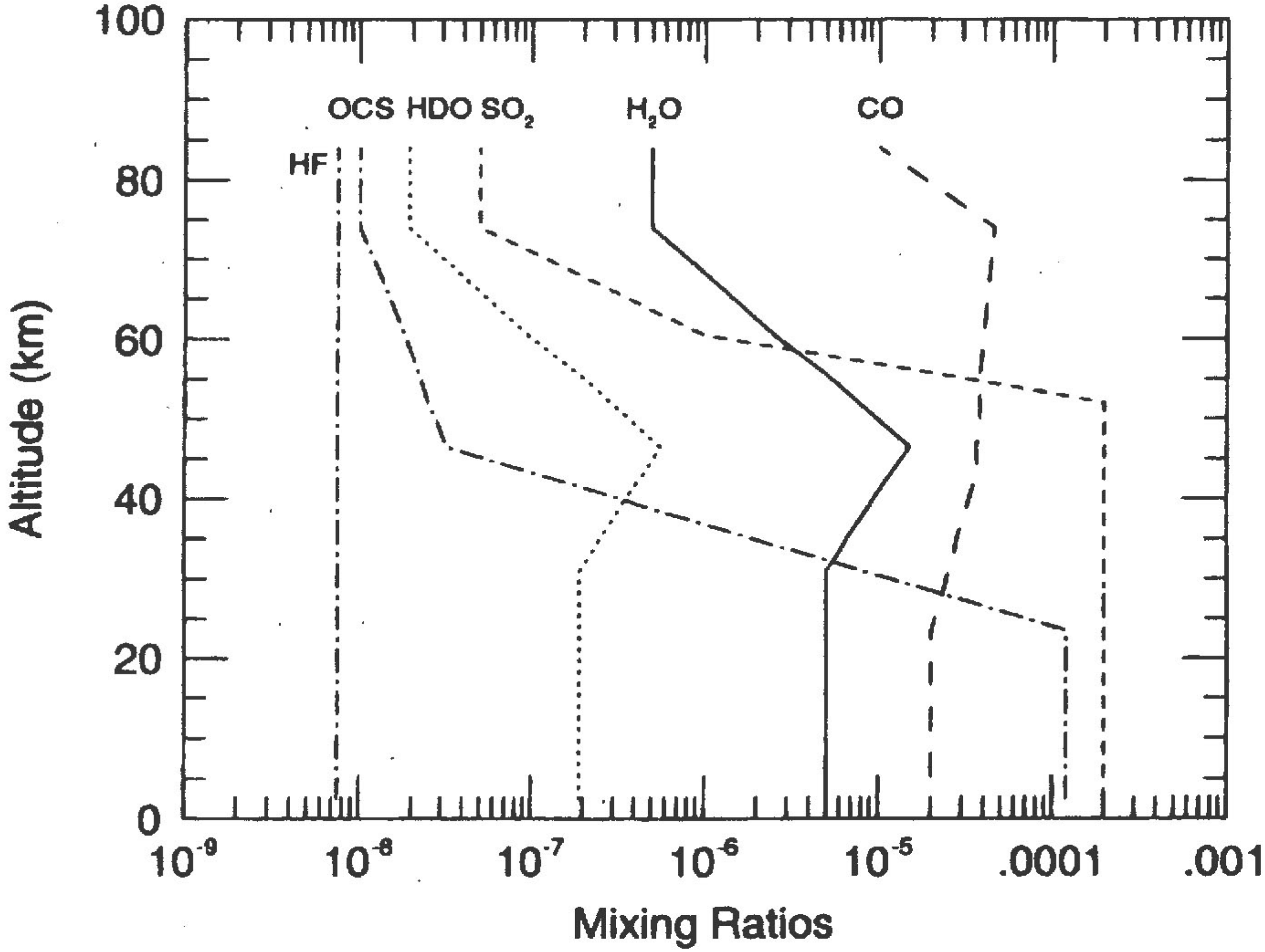

Pollack et al., Icarus 103, 1, 1993

硫黄サイクル

CO_2安定化サイクル

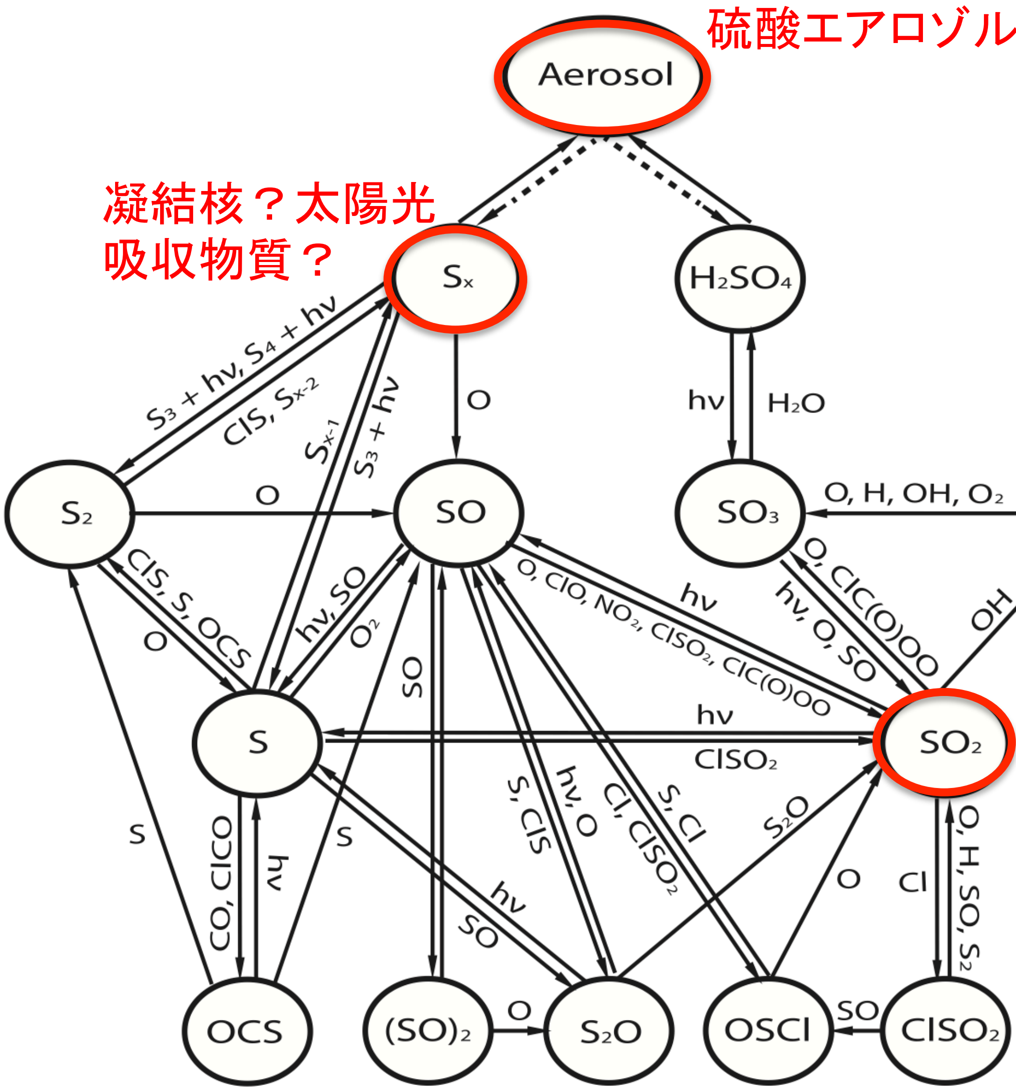

Fig. 9. Important chemical pathways for sulfur species.

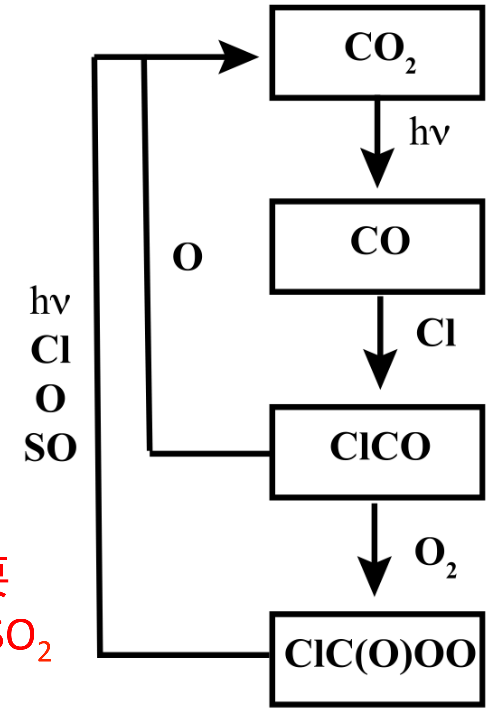

Figure 3. Schematic showing primary pathways for production of CO_2 via chlorine chemistry. The reaction ClCO + O → CO_2 + Cl accounts for 15 and 20% of the column total CO_2 production in the +0.5σ and +2.0σ models from Table 5, respectively.

Zhang et al. (2012)

Mills et al. (2007)

SO, SO_2 profiles above cloud observed by Venus Express solar occultations (Belyaev et al. 2011)

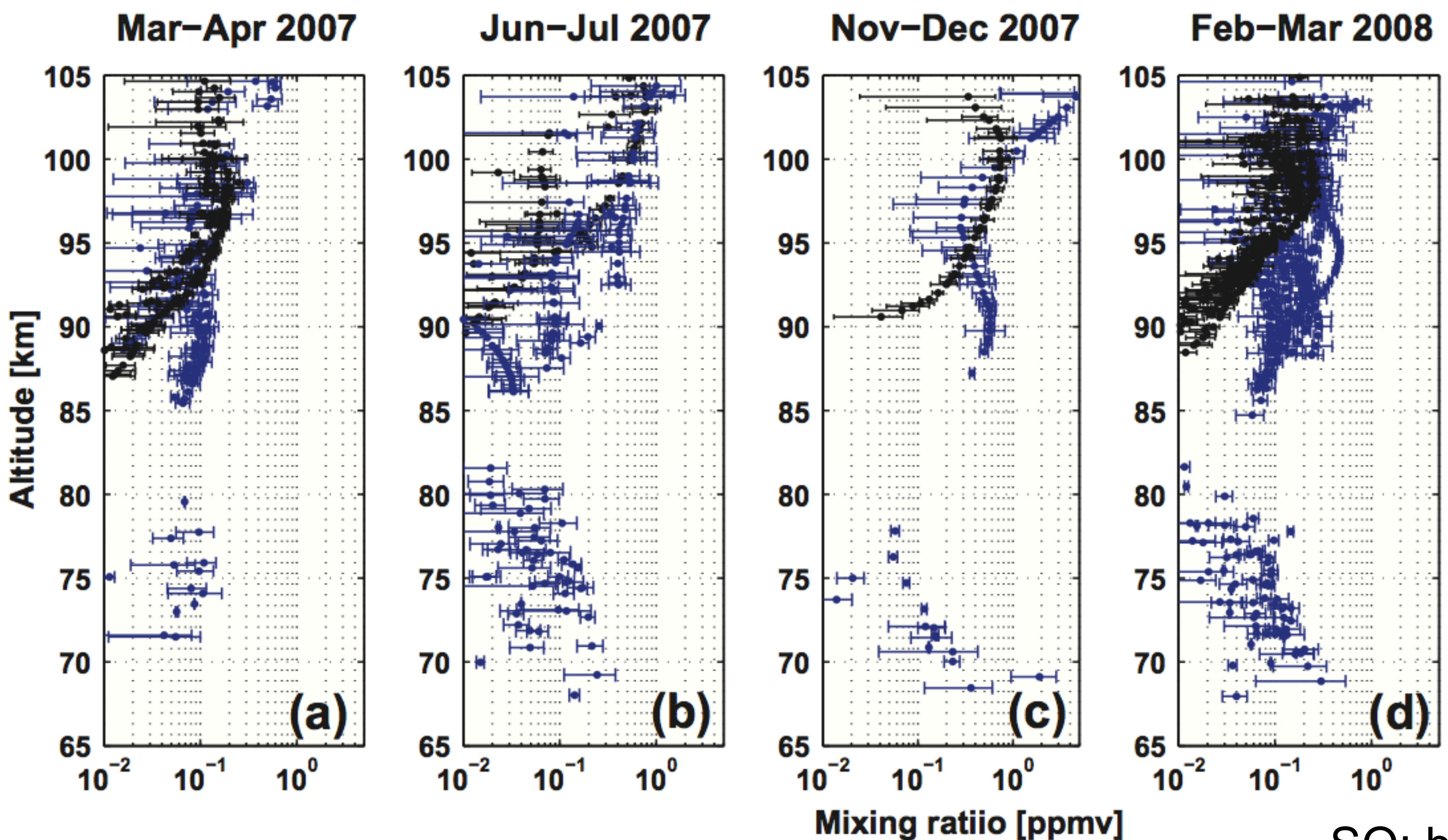

SO: black
SO_2: blue

- Enhancement at high altitudes cannot be explained by traditional photochemical models.

(Zhang et al. 2012)

Artificial H_2SO_4 source added above 90 km:

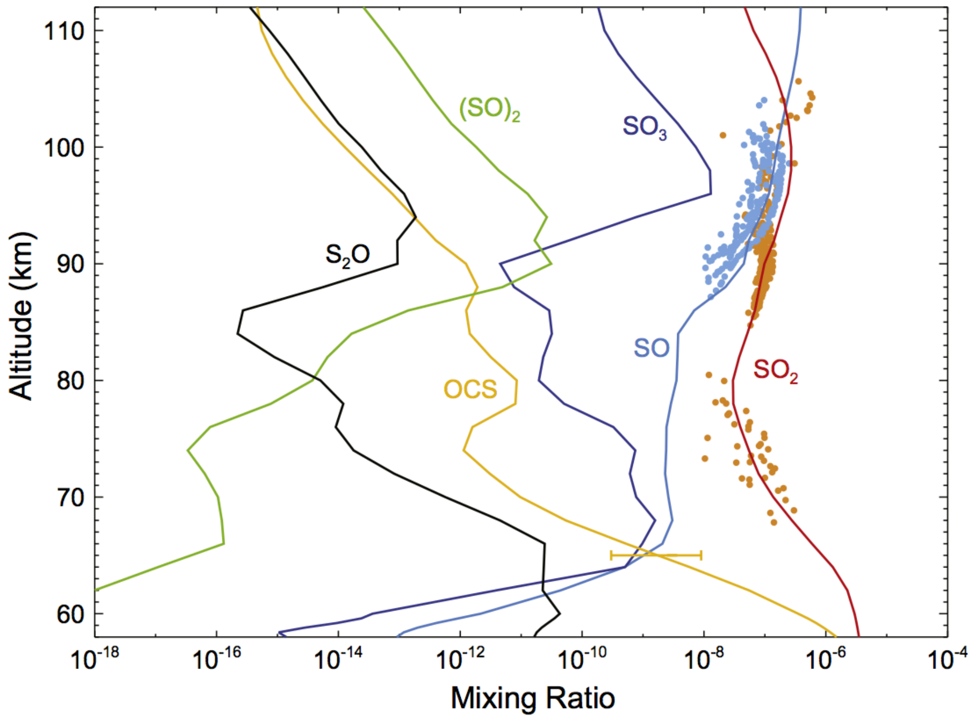

Fig. 8. Same as Fig. 2, for the sulfur oxides. The SO_2 and SO observations with errorbars are from the Belyaev et al. (2012). The temperature at 100 km is 165–170 K for the observations. The OCS measurement (0.3–9 ppb with the mean value of 3 ppb) is from Krasnopolsky (2010).

Transport of cloud particles to the upper atmosphere by winds ?

→ Open question

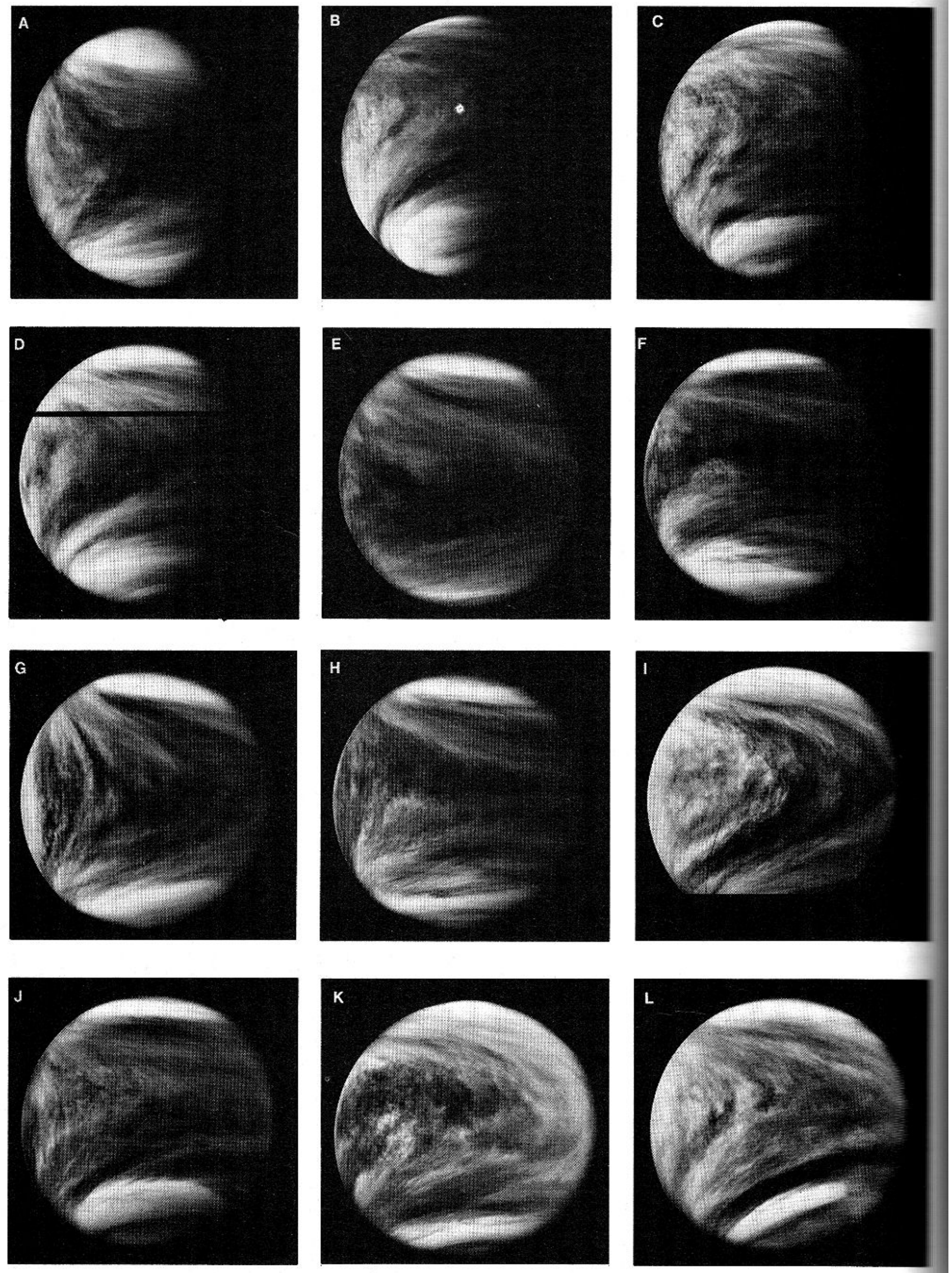

Pioneer Venus
紫外画像(365 nm)

雲の模様の源

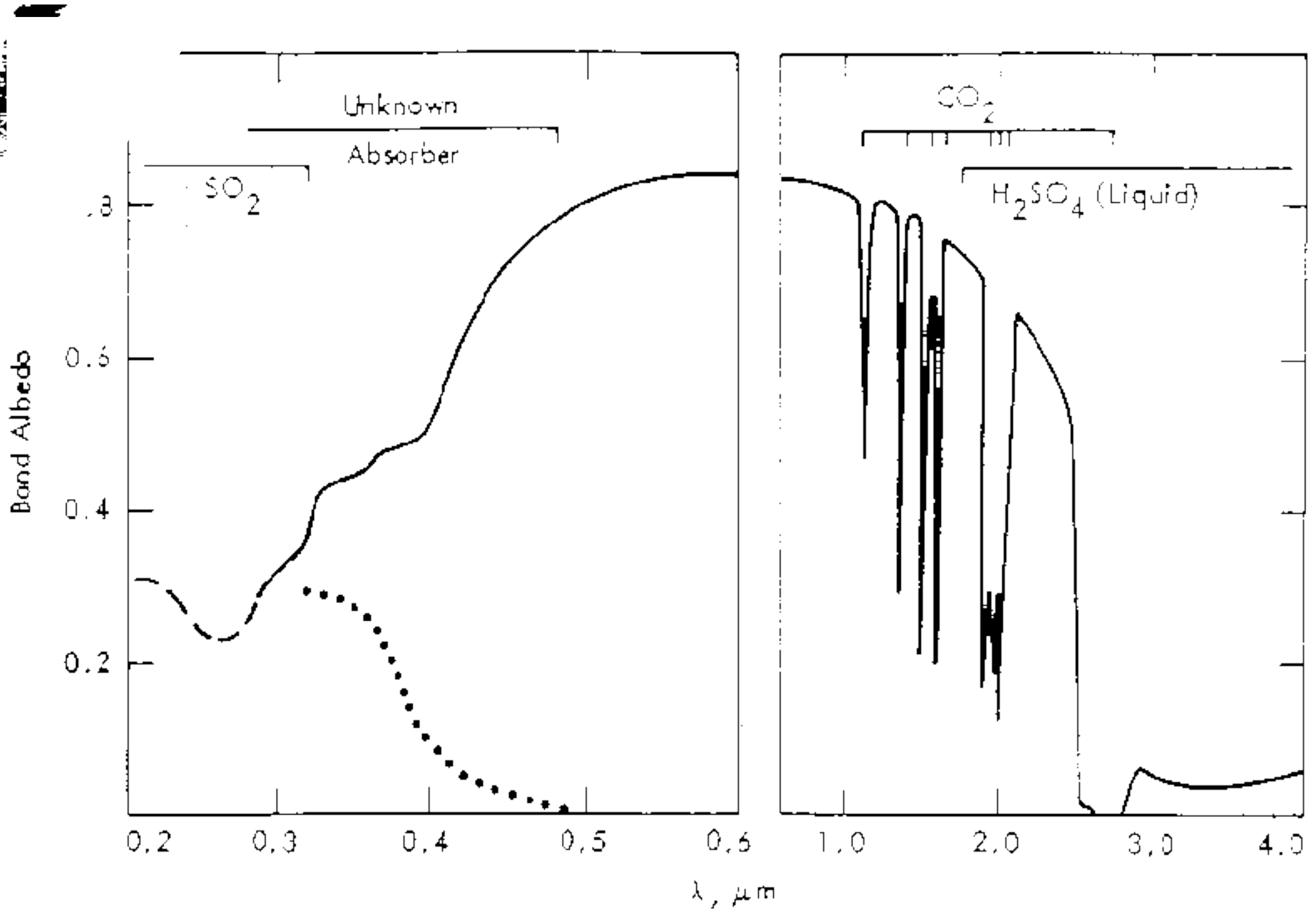

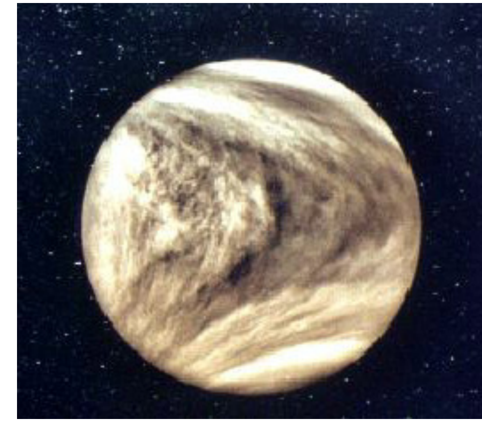

- 遠紫外（<320nm）の吸収はほぼSO_2
- 近紫外（>320nm）の吸収物質の候補：S_3, S_4, S_8, Cl_2, $FeCl_3$, SCl_2, $C_5O_5H_2$, $(NH_4)_2S_2O_5$, $NOHSO_4$, S_2O (Mills et al. 2007)

UV absorption coefficient based on Venera probe measurements

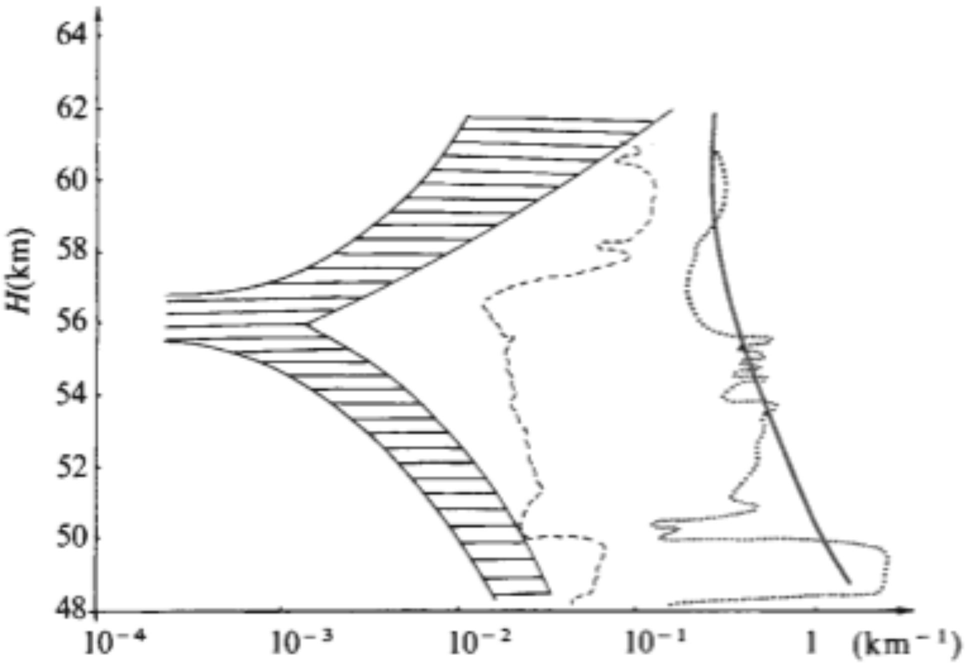

Fig. 2 Observational range in volume absorption coefficient (shaded area) and volume extinction coefficient multiplied by $(1-g)$ (——) as a result of direct computation from the UV photometer data. Also shown are the extinction coefficients multiplied by $(1-g) = 0.2$ (after ref. 13) for mode-1 only (– – –) and total (· · · ·).

Ekonomov et al. (1984)

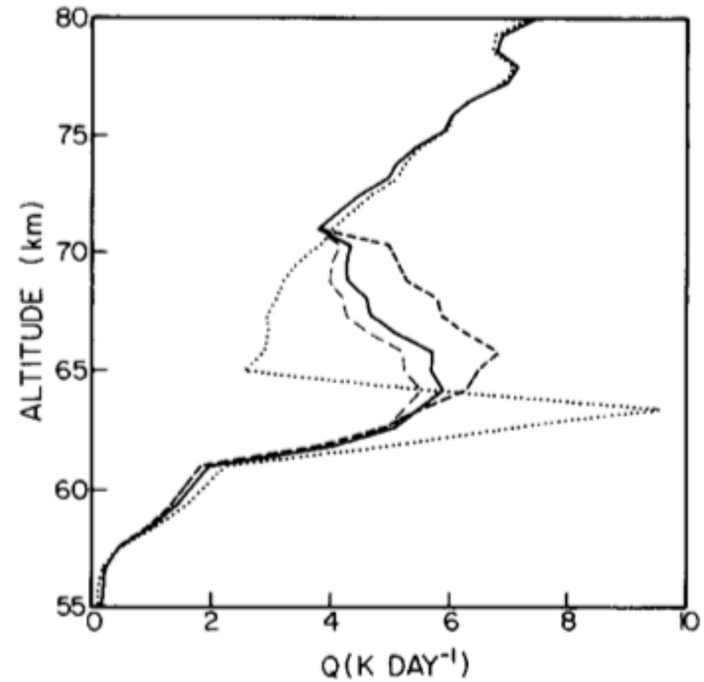

FIG. 11. Global-mean solar heating rates for the nominal, ''high-UV absorber'' case (—) are compared to results obtained for the alternate ''low-UV absorber'' distribution (. . .) described in the text. The total amount of solar flux absorbed by these two distributions is identical. Other curves shown here are those obtained for the extreme cases where the entire planet is covered by a bright (——) or dark (–––) UV feature.

Crisp (1986)

Other vertical transport processes

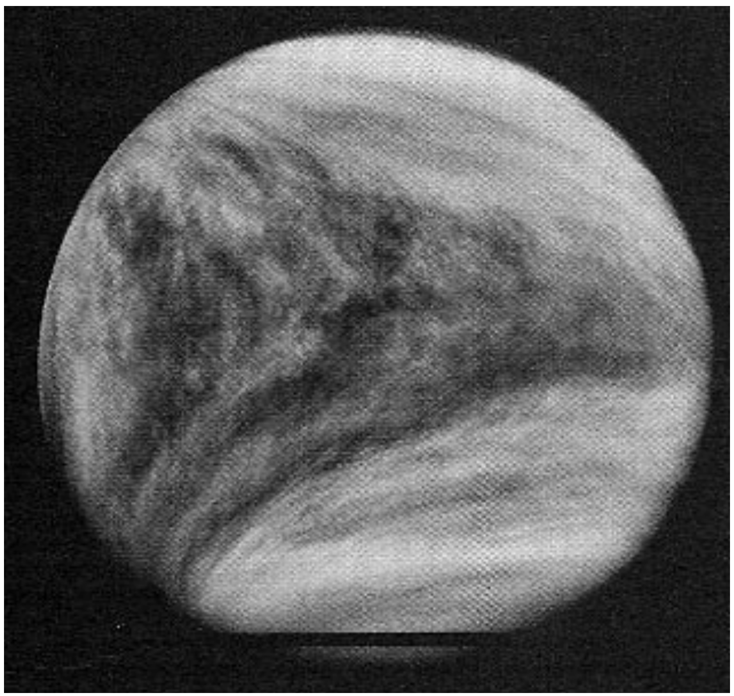

Y-feature
- Kelvin wave?

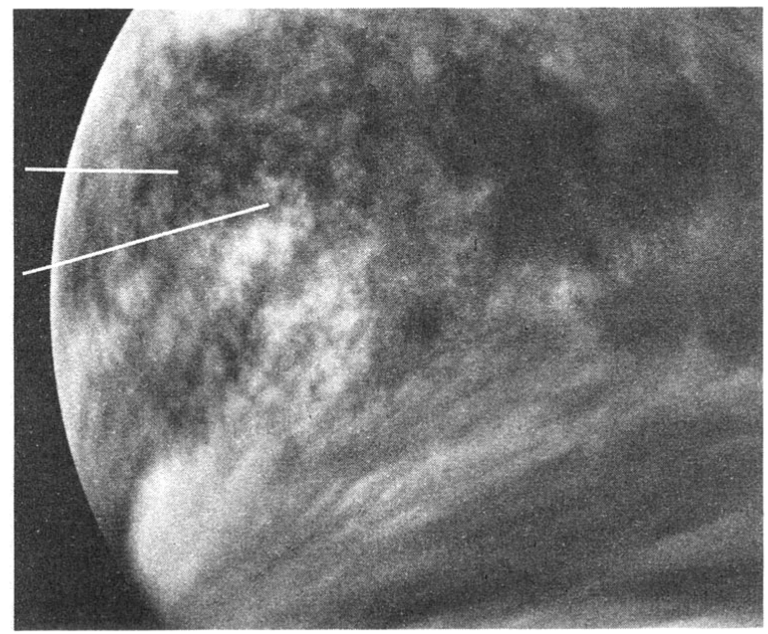

‘Cells’ near sub-solar region

Convection cells near subsolar?

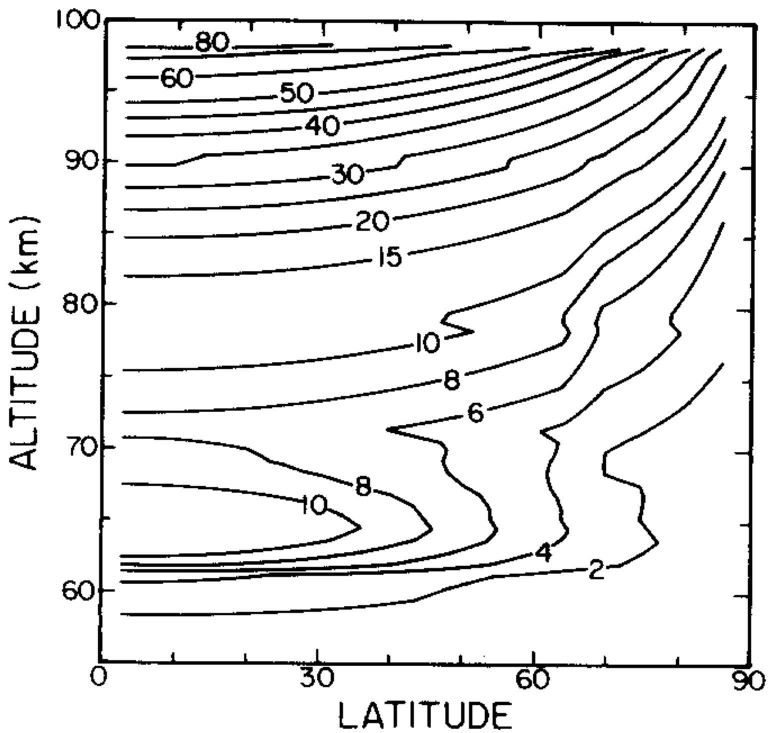

Amplitude of the diurnal component of solar heating (K/day) (Crisp 1986)

Cloud-top water vapor observed by Pioneer Venus (Koukouli et al. 2005)

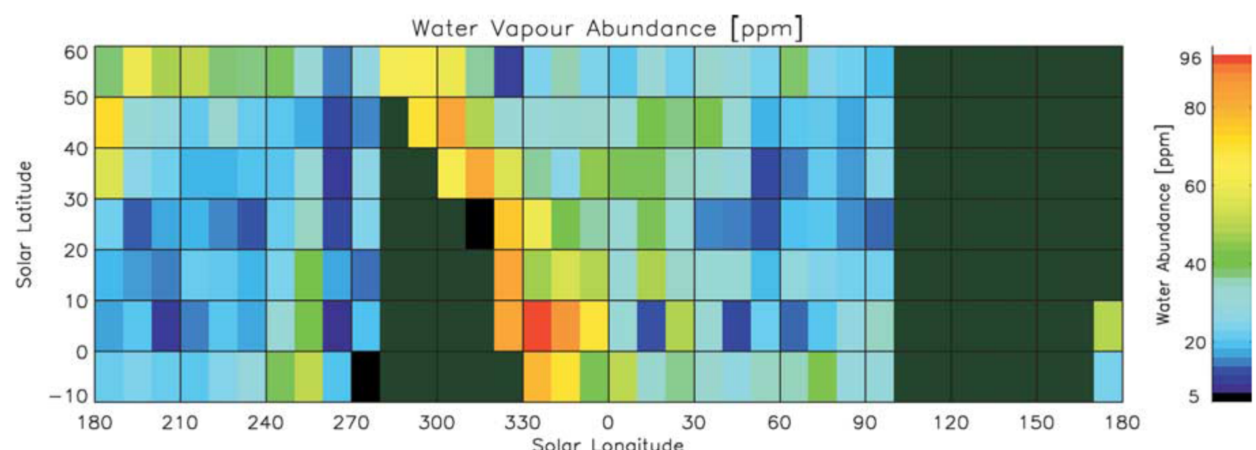

Radio wave generation by lightning discharges ?

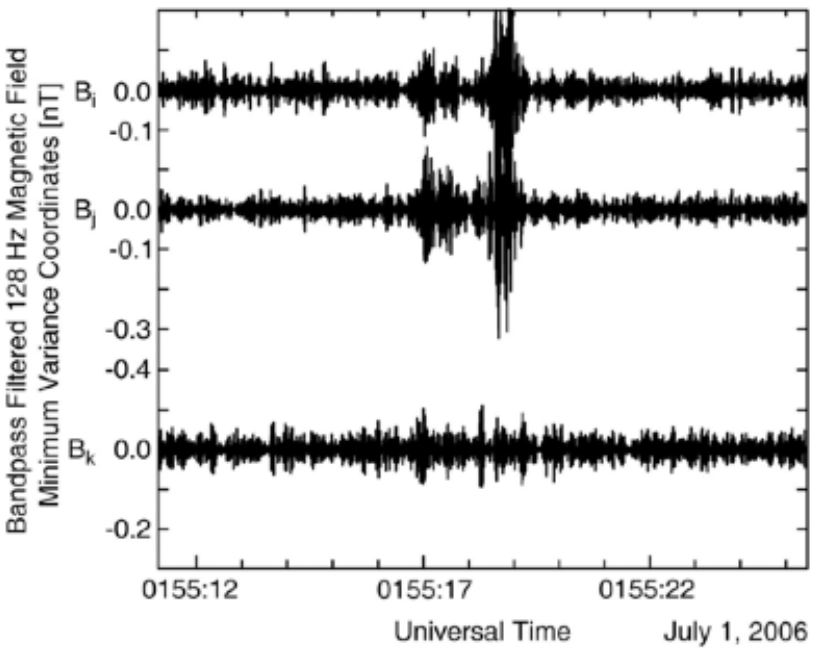

Figure 1. Waveform of 8-ms samples of the magnetic field at periapsis on 1 July 2006, bandpass filtered from 42 to 60 Hz and rotated into principal axis coordinates.

Russell et al. (2008)

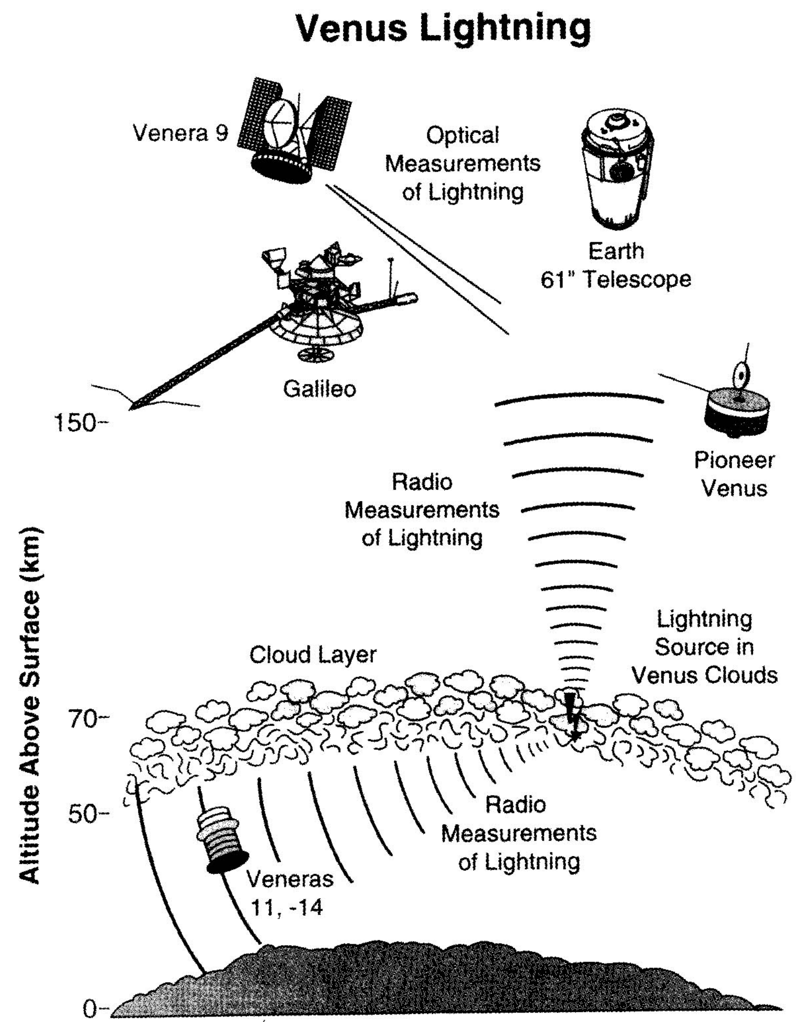

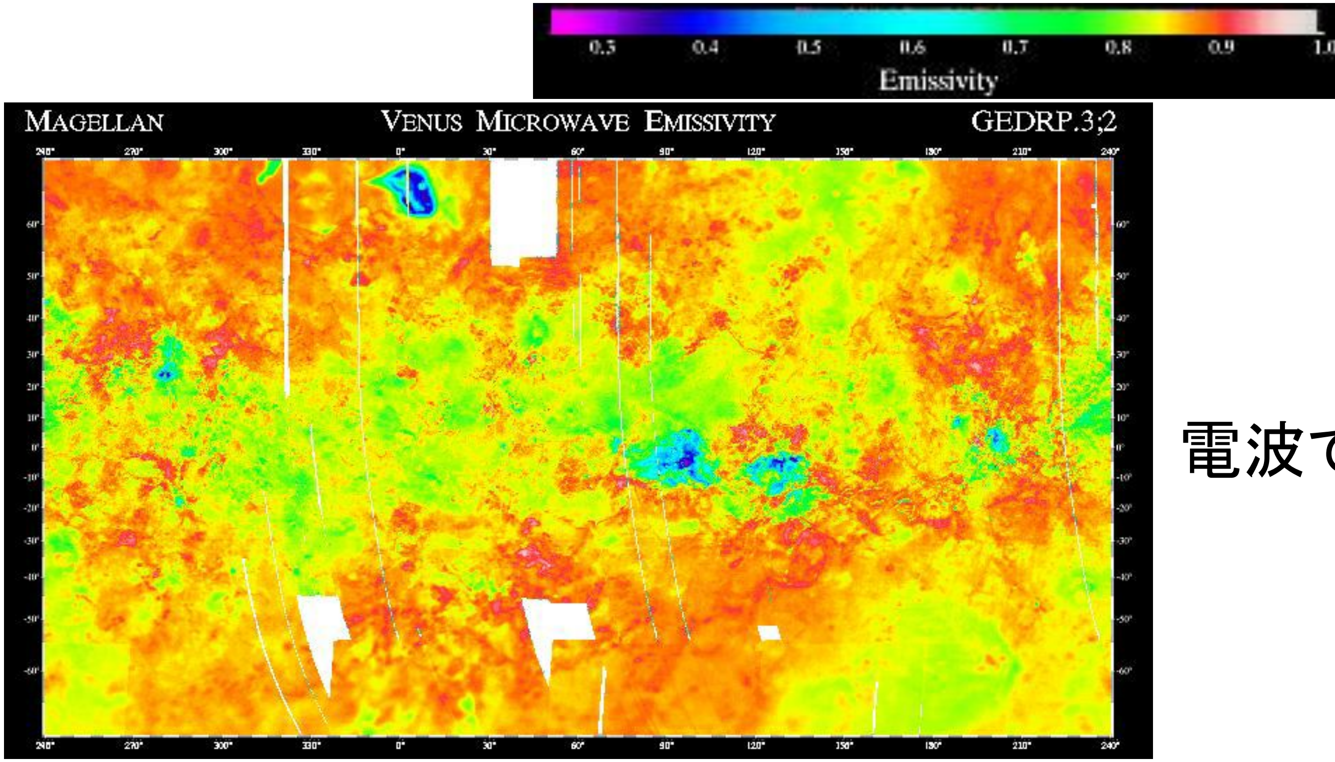
0.3 0.4 0.5 0.6 0.7 0.8 0.9 1.0
Emissivity
MAGELLAN
VENUS MICROWAVE EMISSIVITY
GEDRP.3;2

電波での放射率

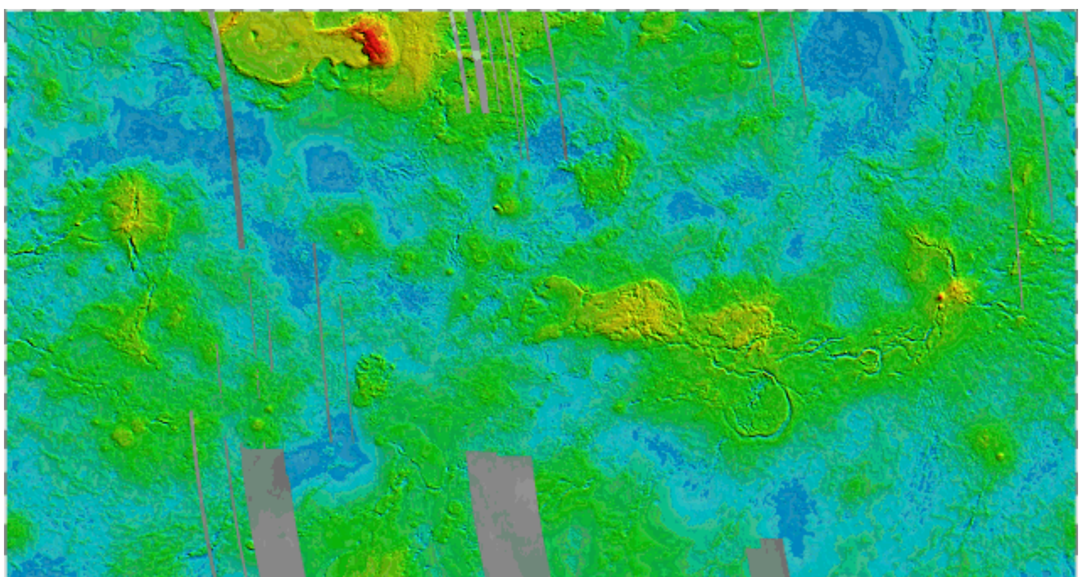

標高

雲アルベドによる気候安定化仮説
(Hashimoto & Abe, 2005)

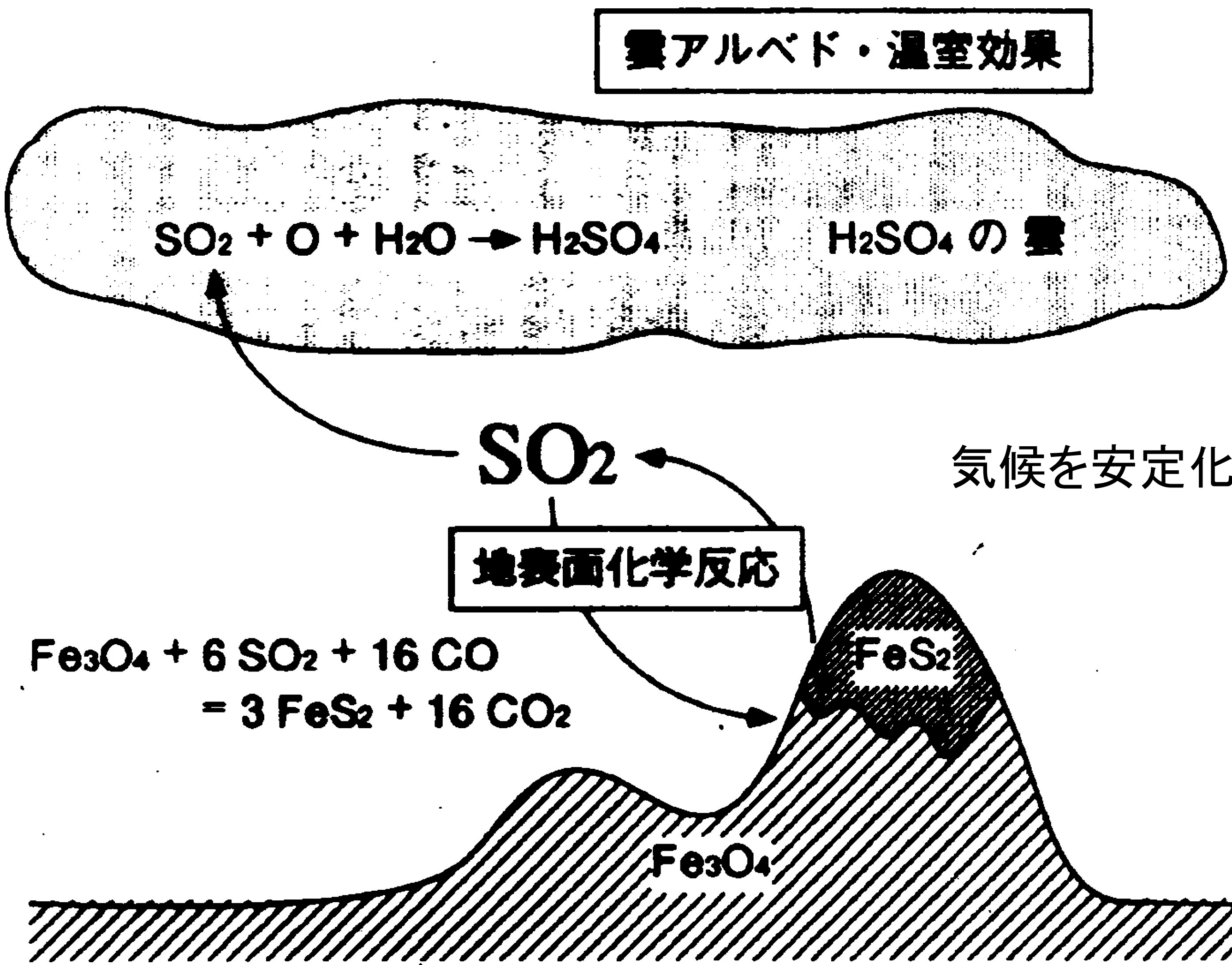

気候を安定化する可能性

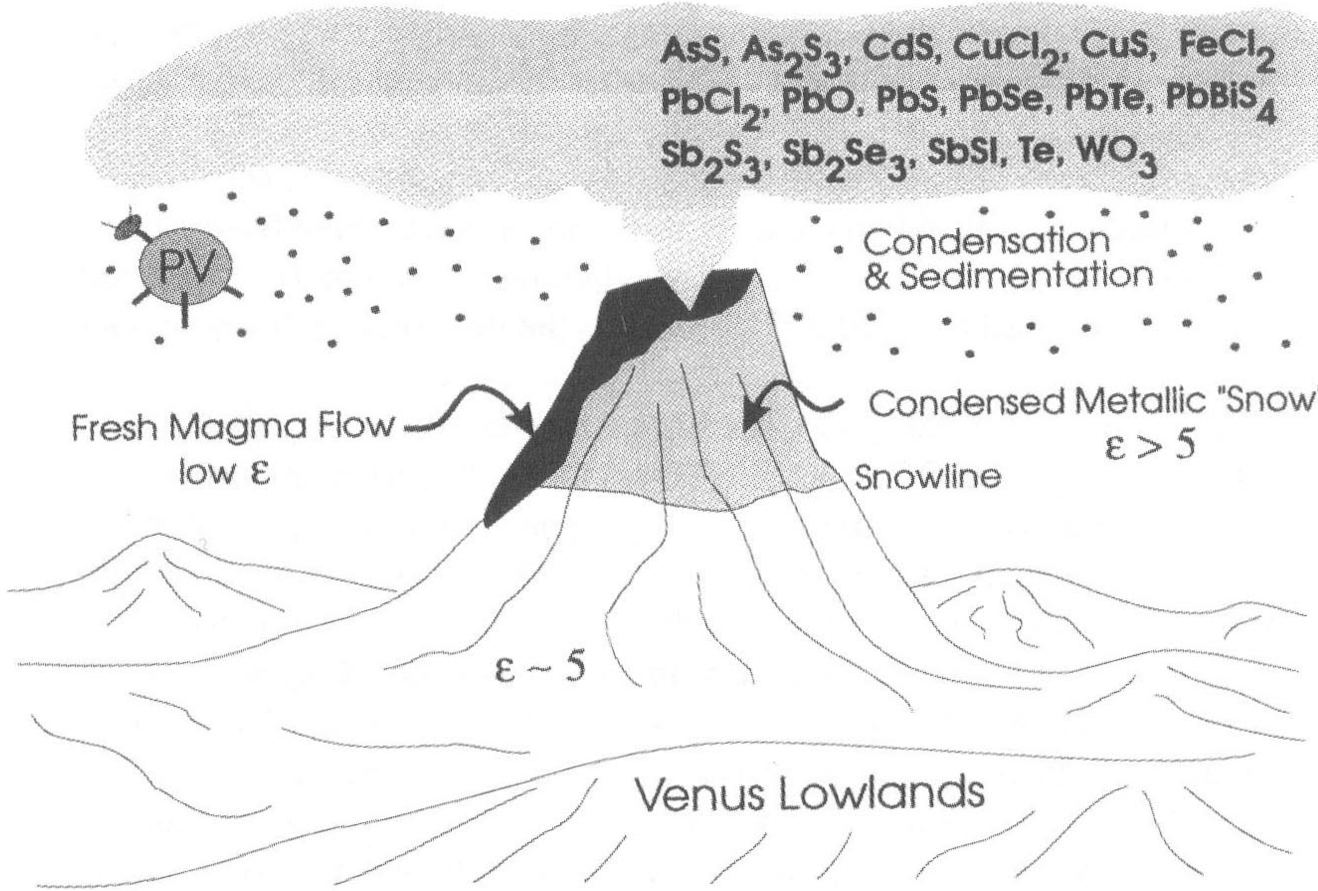

Figure 11. A cartoon schematically illustrating the metallic frost model of Brackett et al. (1995). Volatile metal halides and chalcogenides (i.e., sulfides, selenides, and tellurides), are erupted into the atmosphere of Venus. Some vapor may immediately form aerosol hazes in the near-surface atmosphere of Venus, which may be the cause of the low-altitude hazes observed by two Pioneer Venus entry probes (Ragent and Blamont 1980). Some vapor may immediately snow out and condense out over the entire surface of the planet, and other more volatile species may remain in the near-surface atmosphere. See text for details.

大気-地殻化学相互作用

炭酸塩による大気バッファ仮説

$CaSiO_3 + CO_2 \leftarrow\rightarrow CaCO_3 + SiO_2$

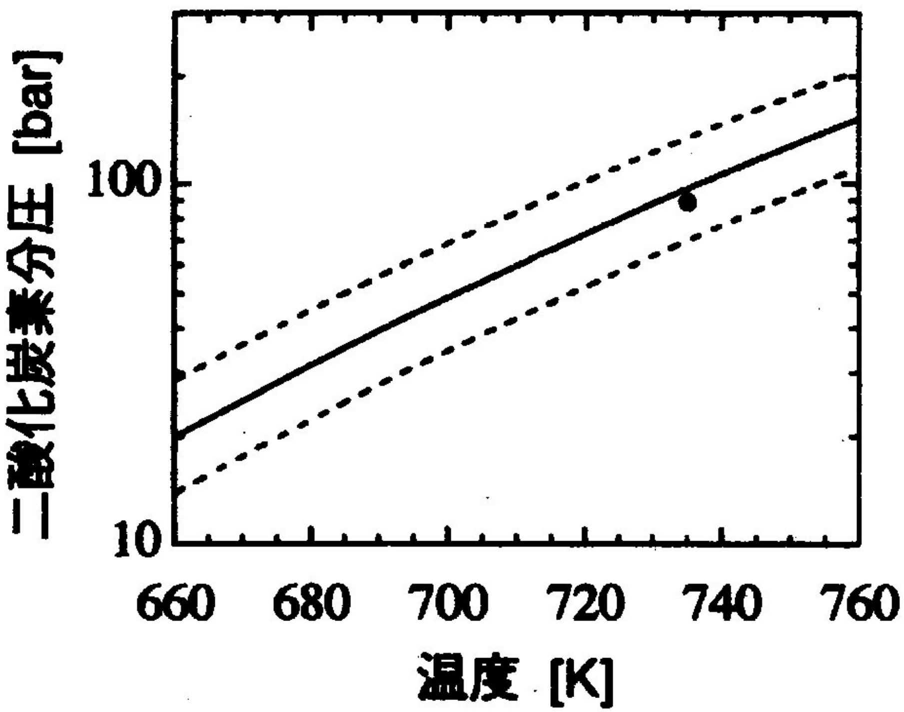

気候を不安定化する可能性

(はしもと･阿部、1998)

Variability of SO_2 above clouds

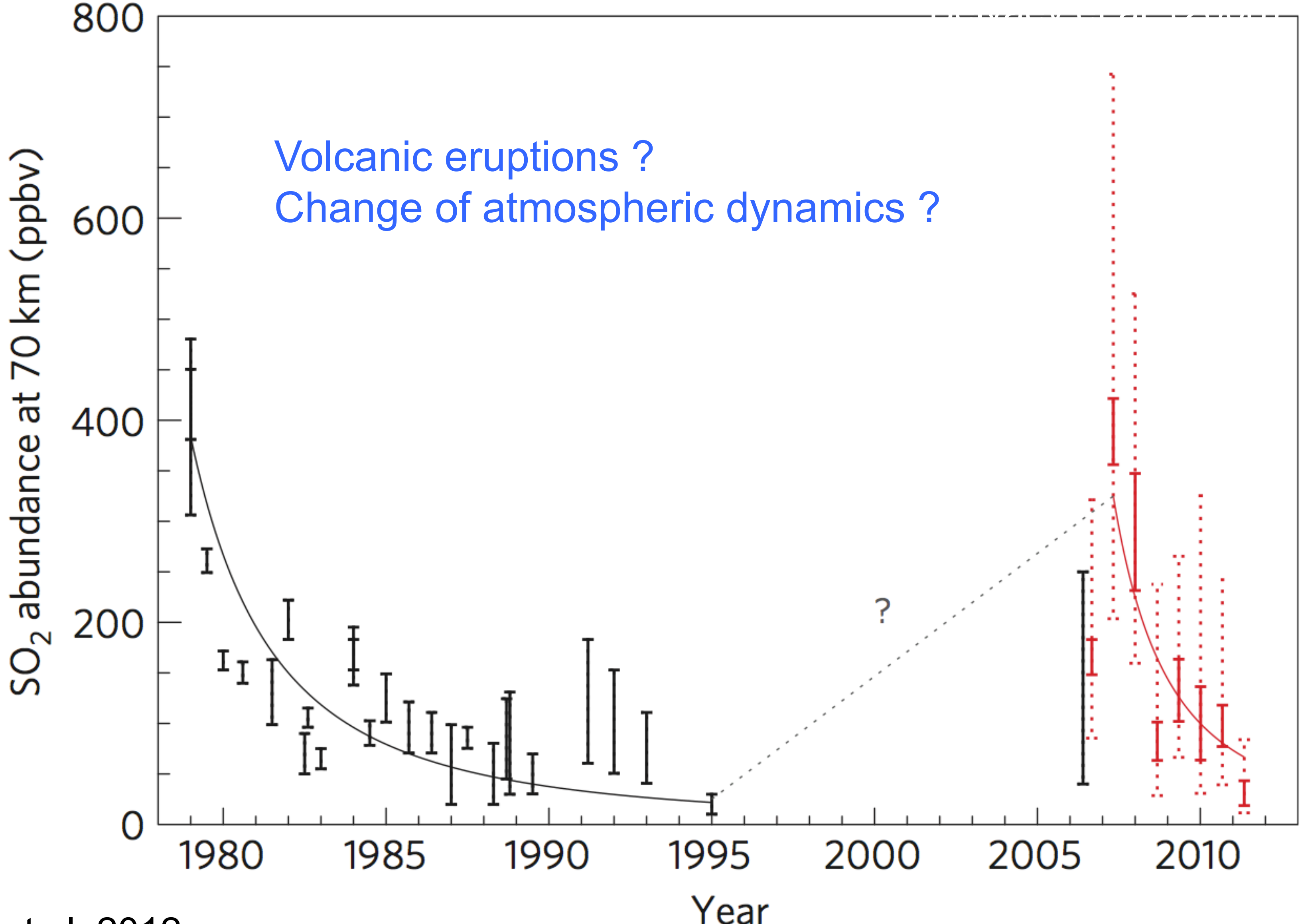

Marcq et al. 2012

Icarus 253 (2015) 1–15

Contents lists available at ScienceDirect

Icarus

journal homepage: www.elsevier.com/locate/icarus

Long-term variations of the UV contrast on Venus observed by the Venus Monitoring Camera on board Venus Express

Y.J. Lee [a,*], T. Imamura [a], S.E. Schröder [b], E. Marcq [c]